Cite as: I. Budin *et al.*, *Science* 10.1126/science.aat7925 (2018).

Viscous control of cellular respiration by membrane lipid composition

Itay Budin[1,2]*, Tristan de Rond[1,3]†, Yan Chen[1,6], Leanne Jade G. Chan[1]‡, Christopher J. Petzold[1,6], Jay D. Keasling[1,2,4-8]*

[1]Joint BioEnergy Institute, 5885 Hollis Street, Emeryville, CA 94608, USA. [2]Department of Chemical and Biomolecular Engineering, University of California, Berkeley, Berkeley CA 94720, USA. [3]Department of Chemistry, University of California, Berkeley, Berkeley, CA 94720, USA. [4]Department of Bioengineering, University of California, Berkeley, Berkeley CA 94720, USA. [5]QB3 Institute, University of California, Berkeley, Berkeley, CA 94270, USA. [6]Biological Systems and Engineering, Lawrence Berkeley National Laboratory, Berkeley, CA 94720, USA. [7]The Novo Nordisk Foundation Center for Sustainability, Technical University of Denmark, Denmark. [8]Center for Synthetic Biochemistry, Institute for Synthetic Biology, Shenzhen Institutes for Advanced Technologies, Shenzhen, China.

*Corresponding author. E-mail: keasling@berkeley.edu (J.D.K.); budin@berkeley.edu (I.B.) †Present address: Scripps Institution of Oceanography, University of California, San Diego, CA, USA. ‡Present address: Calico Life Sciences, South San Francisco, CA, USA.

Lipid composition determines the physical properties of biological membranes and can vary substantially between and within organisms. We describe a specific role for the viscosity of energy-transducing membranes in cellular respiration. Engineering of fatty acid biosynthesis in *Escherichia coli* allowed us to titrate inner membrane viscosity across a 10-fold range by controlling the abundance of unsaturated or branched lipids. These fluidizing lipids tightly controlled respiratory metabolism, an effect that can be explained with a quantitative model of the Electron Transport Chain (ETC) that features diffusion-coupled reactions between enzymes and electron carriers (quinones). Lipid unsaturation also modulated mitochondrial respiration in engineered budding yeast strains. Thus, diffusion in the ETC may serve as an evolutionary constraint for lipid composition in respiratory membranes.

Cell membranes contain a multitude of distinct lipid components, but understanding how specific lipids influence biological function is challenged by limited tools for their manipulation in vivo (*1*). Lipids can determine the physical characteristics of membranes (*2*), such as their viscosity, and these properties are homeostatically maintained by cells (*3*). In a classic example (fig. S1), the bacterium *E. coli* increases the proportion of phospholipid acyl chains with double bonds (unsaturation) with decreasing growth temperatures, thereby maintaining a constant membrane viscosity (*4*). Similar lipid adaptations have been widely observed across organisms (*5*), suggesting that universal processes are mediated by membrane viscosity.

To investigate functions for membrane viscosity in vivo, we used metabolic engineering strategies to genetically modulate lipid composition in *E. coli* (fig. S2). FabB (β-ketoacyl-[acyl carrier protein] synthase I) carries out the rate-limiting step (*6*) for production of unsaturated fatty acids (UFAs) during fatty acid (FA) biosynthesis (Fig. 1A). We replaced the chromosomal copy of *fabB* with one under control of an *L*-arabinose-induced promoter (P_{BAD}) in a strain background that allows for titratable and homogenous expression (*7*, *8*). After further tuning FabB levels with Shine-Dalgarno Sequence variants (fig. S2C), we generated strains with controllable UFA amounts ranging from ~15% [the minimum amount for survival (*9*)] to ~ 80% of all FAs at 37°C (Fig. 1B). This modulation resulted primarily from the substitution of palmitate (C16:0) with vaccinate (C18:1) acyl chains (fig. S3A), which was observed in all phospholipid species (fig. S3B) and maintained throughout exponential growth (fig. S3D). Membrane ordering, as measured by steady-state anisotropy of diphenyl-hexatriene (DPH), steadily decreased with increasing lipid unsaturation in both inner membrane vesicles and protein-free liposomes (Fig. 1C). To estimate the effect of lipid unsaturation on membrane microviscosity, we measured diffusion coefficients of a nitrobenzoxadiazole (NBD) conjugated phosphoethanolamine (PE) in giant *E. coli* inner membrane vesicles (GEVs) using Fluorescence Recovery After Photobleaching (FRAP) (Fig. 1D). From these data, viscosities were derived using the Saffman-Delbrück approximation (*10*) and showed a 10-fold range (~2 to 20 poise) as UFA content was modulated.

To identify physiological functions for UFAs, we correlated exponential growth rates with sampled lipid compositions in cells producing various amounts of FabB (Fig. 2A). Growth rates generally featured a biphasic dependence on lipid unsaturation: A sharp fitness cliff leading to a cessation of cell growth at low UFA levels (15-20% at 37°C, regime I), followed by increasing growth rates with higher UFA content (regime II). Regime I corresponded to the minimum amount of UFAs required (e.g., in fig. S1) and was observed under all conditions. In contrast, regime II was dependent on media with non-fermentable carbon sources, where growth is tightly coupled to ATP production through the Electron

Downloaded from http://science.sciencemag.org/ on October 25, 2018

Transport Chain (ETC) (*11*). Under fermentation conditions, when cells depend on glycolysis and are resistant to respiratory uncouplers (fig. S4D), growth rates were unaffected by UFAs in regime II (Fig. 2A). An analysis of stress response factors (Fig. 2B) showed that that low UFA levels caused both an Oxidative Stress Response (OSR), which can result from ETC inhibition (*12*), and a Heat Shock Response (HSR), which is activated by misfolded proteins (*13*). However, HSR activation occurred only as membranes approached a gel phase transition at the growth temperature (fig. S5B), and coincided with the mislocalization of membrane proteins (fig. S5C) and defects in cell division (fig. S5D). We therefore concluded that increasing proportions of saturated lipids trigger envelope stress as membranes become highly ordered (regime I), but also have a second, respiratory role over a broader range of stoichiometry (regime II).

When titrating FA synthesis, cellular respiration rates were tightly coupled to changes in unsaturated lipid content (Fig. 2C). This effect was independent of electron donor (for example, succinate or glycerol), electron acceptor (oxygen or nitrate), proton motive force (PMF) uncoupling, oxygen concentration (fig. S6A), and growth stage (fig. S6B). Wild-type cells overproducing UFAs through *fabB* overexpression or deletion of the regulator *fabR* similarly showed increased respiratory rates (fig. S6C). Under glucose fermentation, low lipid unsaturation led to the accumulation of pyruvate and lactate as secreted organic acids and a depletion of succinate. Such a mixed acid fermentation profile is consistent with ETC inhibition (fig. S6D).

To test if respiratory regulation occurs through a physical effect, we engineered a heterologous system for controlling membrane viscosity based on branched-chain fatty acid (BCFA) synthesis (Fig. 2D). Introduction of the *bkd* operon (for biosynthesis of β-ketoacids) and *fabH* (for initiation of BCFA synthesis) from *Bacillus subtilis* led to the accumulation of BCFAs in membrane lipids (fig. S7A), especially when amounts of UFA were low (fig. S7B). BCFA biosynthesis fluidized membranes (fig. S7C) and rescued growth defects from low lipid unsaturation (fig. S7D), even at amounts of UFAs that were otherwise lethal (fig. S7E). Uncoupled respiration rates were increased by BCFAs in addition to UFAs, and the effects of both fatty acid species were preserved in isolated membrane vesicles (Fig. 2E).

We considered three mechanisms by which membrane viscosity could control ETC function. First, substrate uptake could be dependent on membrane properties, especially the passive permeation of oxygen. However, lipids act on respiration independently of substrate and oxygen concentrations (fig. S6A). Alternatively, viscosity could affect individual ETC enzymes, but their partial activities with soluble substrates were not inhibited by saturated lipids (fig. S6E). Lastly, we considered whether viscosity mediates collisions between electron carriers (ubiquinone) and enzyme complexes in the ETC, since a rate dependence on solvent viscosity is a hallmark of diffusion-limited reactions (*14*). Based on the pool behavior of quinones (*15*, *16*), their diffusion between complexes has been proposed to be rate-limiting in mitochondrial respiration (*17*, *18*), but this concept was disputed (*19*, *20*).

To investigate the role of diffusion in cellular respiration, we developed a model of the *E. coli* ETC based on the Brownian motion of membrane components and their collision-mediated reactions (Fig. 3A, fig. S8). As inputs, we combined activities of purified ETC enzymes - dehydrogenases (DHs) and terminal oxidases (TOs) - with measurements of their absolute abundances using quantitative mass spectrometry (Supplementary Information) and their organization into homotypic domains as previously described (*21*, *22*). Whole cell simulations were then carried out to quantify the rate of electron transfer as a function of ubiquinone diffusivity. To measure this parameter, we used FRAP experiments with an NBD-conjugated ubiquinone (NBD-UQ, fig. S9), thereby defining lipid-dependent diffusion coefficients (Fig. 3B).

Our model predicted that ubiquinone diffusivity controls respiratory flux in membranes spanning the tested range of lipid compositions. Diffusion control was measured by quinone anisotropy, with reduced electron carriers becoming depleted in the vicinity of TOs (Fig. 3C and movie S1). As diffusion increased, the quinone pool became well-mixed and rates were increasingly determined by enzyme activities (fig. S8B). Simulations matched measured respiratory rates when enzymes were modeled as domains of 10 to 30 proteins (Fig. 3D), consistent with their reported organization in cells (*21*). Simulations also predicted changes to respiratory rates upon inhibition of ETC enzymes (Fig. 3E), which reduces the rate dependence on diffusion, and during genetic titration of TO abundance (Fig. 3F), which modulates the average diffusion distance for a reactive collision.

As in bacteria, respiration in eukaryotic mitochondria is also dependent on quinone-mediated electron transfer. In animal models, correlations between mitochondrial FA composition and metabolic rate have been observed between species (*23*), and membrane-fluidizing steroids have been shown to promote respiration (*24*). To test whether lipid composition controls mitochondrial respiration, we used a set of constitutive promoters to manipulate Ole1 (stearoyl-CoA-9-desaturase) levels in *Saccharomyces cerevisiae* (Fig. 4A). In strains that showed regular mitochondrial morphology (fig. S10A), greater lipid unsaturation led to increased respiratory activity but, as in *E. coli*, did not inhibit fermentative metabolism or growth (fig. S10, B and C). In isolated mitochondria, UFA content controlled the rate of respiration coupled to ADP-phosphorylation (State 3) and uncoupled (State 3u) from the PMF (Fig. 4B).

The role for diffusion in respiration provides a functional

Downloaded from http://science.sciencemag.org/ on October 25, 2018

rationale for variations in lipids within and between cells. In eukaryotes, lipid species that increase membrane viscosity – sterols and sphingolipids – are depleted from energy-transducing membranes (*25*). In prokaryotes, analogous rigidifying lipids, such as hopanoids and archaeal ether lipids, are associated with niches where the robustness of the membrane as a permeability barrier is paramount over rapid metabolic activity (*26*). Such a trade-off is evident in *E. coli*, which eliminates lipid unsaturation through cyclopropanation during stationary phase to survive in acidic conditions (*27*). Localizing ETCs to fluid internal membranes while maintaining rigid outer membranes could thus have served as an advantage during the evolution of dedicated metabolic organelles. In some mitochondria, ETCs are additionally organized into supercomplexes of respiratory enzymes (*28*, *29*). In our simulations, tethering of DH and TO enzymes increased respiration rates and reduced anisotropy in the quinone pool (fig. S11, movie S2, supplementary text). A diffusion-coupled reaction model could therefore be important for understanding how the interplay between lipid composition, enzymatic activity, and membrane organization dictates respiratory function in a wide range of systems.

REFERENCES AND NOTES

1. E. Muro, G. E. Atilla-Gokcumen, U. S. Eggert, Lipids in cell biology: How can we understand them better? *Mol. Biol. Cell* **25**, 1819–1823 (2014). doi:10.1091/mbc.e13-09-0516 Medline
2. T. Harayama, H. Riezman, Understanding the diversity of membrane lipid composition. *Nat. Rev. Mol. Cell Biol.* **19**, 281–296 (2018). doi:10.1038/nrm.2017.138 Medline
3. R. Covino, S. Ballweg, C. Stordeur, J. B. Michaelis, K. Puth, F. Wernig, A. Bahrami, A. M. Ernst, G. Hummer, R. Ernst, A Eukaryotic Sensor for Membrane Lipid Saturation. *Mol. Cell* **63**, 49–59 (2016). doi:10.1016/j.molcel.2016.05.015 Medline
4. M. Sinensky, Homeoviscous adaptation—A homeostatic process that regulates the viscosity of membrane lipids in Escherichia coli. *Proc. Natl. Acad. Sci. U.S.A.* **71**, 522–525 (1974). doi:10.1073/pnas.71.2.522 Medline
5. J. R. Hazel, Thermal adaptation in biological membranes: Is homeoviscous adaptation the explanation? *Annu. Rev. Physiol.* **57**, 19–42 (1995). doi:10.1146/annurev.ph.57.030195.000315 Medline
6. Y. Feng, J. E. Cronan, Escherichia coli unsaturated fatty acid synthesis: Complex transcription of the fabA gene and in vivo identification of the essential reaction catalyzed by FabB. *J. Biol. Chem.* **284**, 29526–29535 (2009). doi:10.1074/jbc.M109.023440 Medline
7. A. Khlebnikov, K. A. Datsenko, T. Skaug, B. L. Wanner, J. D. Keasling, Homogeneous expression of the P(BAD) promoter in Escherichia coli by constitutive expression of the low-affinity high-capacity AraE transporter. *Microbiology* **147**, 3241–3247 (2001). doi:10.1099/00221287-147-12-3241 Medline
8. M. A. Kay, C. Y. He, Z. Y. Chen, A robust system for production of minicircle DNA vectors. *Nat. Biotechnol.* **28**, 1287–1289 (2010). doi:10.1038/nbt.1708 Medline
9. J. E. Cronan Jr., E. P. Gelmann, An estimate of the minimum amount of unsaturated fatty acid required for growth of Escherichia coli. *J. Biol. Chem.* **248**, 1188–1195 (1973). Medline
10. P. G. Saffman, M. Delbrück, Brownian motion in biological membranes. *Proc. Natl. Acad. Sci. U.S.A.* **72**, 3111–3113 (1975). doi:10.1073/pnas.72.8.3111 Medline
11. K. B. Andersen, K. von Meyenburg, Are growth rates of Escherichia coli in batch cultures limited by respiration? *J. Bacteriol.* **144**, 114–123 (1980). Medline
12. A. N. Woodmansee, J. A. Imlay, Reduced flavins promote oxidative DNA damage in non-respiring Escherichia coli by delivering electrons to intracellular free iron. *J. Biol. Chem.* **277**, 34055–34066 (2002). doi:10.1074/jbc.M203977200 Medline
13. T. Yura, K. Nakahigashi, Regulation of the heat-shock response. *Curr. Opin. Microbiol.* **2**, 153–158 (1999). doi:10.1016/S1369-5274(99)80027-7 Medline
14. A. C. Brouwer, J. F. Kirsch, Investigation of diffusion-limited rates of chymotrypsin reactions by viscosity variation. *Biochemistry* **21**, 1302–1307 (1982). doi:10.1021/bi00535a030 Medline
15. A. Kröger, M. Klingenberg, The kinetics of the redox reactions of ubiquinone related to the electron-transport activity in the respiratory chain. *Eur. J. Biochem.* **34**, 358–368 (1973). doi:10.1111/j.1432-1033.1973.tb02767.x Medline
16. P. R. Rich, A generalised model for the equilibration of quinone pools with their biological donors and acceptors in membrane-bound electron transfer chains. *FEBS Lett.* **130**, 173–178 (1981). doi:10.1016/0014-5793(81)81113-1 Medline
17. B. Chazotte, C. R. Hackenbrock, Lateral diffusion as a rate-limiting step in ubiquinone-mediated mitochondrial electron transport. *J. Biol. Chem.* **264**, 4978–4985 (1989). Medline
18. S. Gupte, E. S. Wu, L. Hoechli, M. Hoechli, K. Jacobson, A. E. Sowers, C. R. Hackenbrock, Relationship between lateral diffusion, collision frequency, and electron transfer of mitochondrial inner membrane oxidation-reduction components. *Proc. Natl. Acad. Sci. U.S.A.* **81**, 2606–2610 (1984). doi:10.1073/pnas.81.9.2606 Medline
19. C. Bianchi, M. L. Genova, G. Parenti Castelli, G. Lenaz, The mitochondrial respiratory chain is partially organized in a supercomplex assembly: Kinetic evidence using flux control analysis. *J. Biol. Chem.* **279**, 36562–36569 (2004). doi:10.1074/jbc.M405135200 Medline
20. R. Fato, M. Battino, M. Degli Esposti, G. Parenti Castelli, G. Lenaz, Determination of partition and lateral diffusion coefficients of ubiquinones by fluorescence quenching of n-(9-anthroyloxy)stearic acids in phospholipid vesicles and mitochondrial membranes. *Biochemistry* **25**, 3378–3390 (1986). doi:10.1021/bi00359a043 Medline
21. I. Llorente-Garcia, T. Lenn, H. Erhardt, O. L. Harriman, L.-N. Liu, A. Robson, S.-W. Chiu, S. Matthews, N. J. Willis, C. D. Bray, S.-H. Lee, J. Y. Shin, C. Bustamante, J. Liphardt, T. Friedrich, C. W. Mullineaux, M. C. Leake, Single-molecule in vivo imaging of bacterial respiratory complexes indicates delocalized oxidative phosphorylation. *Biochim. Biophys. Acta* **1837**, 811–824 (2014). doi:10.1016/j.bbabio.2014.01.020 Medline
22. T. Lenn, M. C. Leake, C. W. Mullineaux, Clustering and dynamics of cytochrome bd-I complexes in the Escherichia coli plasma membrane in vivo. *Mol. Microbiol.* **70**, 1397–1407 (2008). doi:10.1111/j.1365-2958.2008.06486.x Medline
23. M. D. Brand, P. Couture, P. L. Else, K. W. Withers, A. J. Hulbert, Evolution of energy metabolism. Proton permeability of the inner membrane of liver mitochondria is greater in a mammal than in a reptile. *Biochem. J.* **275**, 81–86 (1991). doi:10.1042/bj2750081 Medline
24. M. J. Torres, K. A. Kew, T. E. Ryan, E. R. Pennington, C.-T. Lin, K. A. Buddo, A. M. Fix, C. A. Smith, L. A. Gilliam, S. Karvinen, D. A. Lowe, E. E. Spangenburg, T. N. Zeczycki, S. R. Shaikh, P. D. Neufer, 17β-Estradiol Directly Lowers Mitochondrial Membrane Microviscosity and Improves Bioenergetic Function in Skeletal Muscle. *Cell Metab.* **27**, 167–179.e7 (2018). doi:10.1016/j.cmet.2017.10.003 Medline
25. G. van Meer, D. R. Voelker, G. W. Feigenson, Membrane lipids: Where they are and how they behave. *Nat. Rev. Mol. Cell Biol.* **9**, 112–124 (2008). doi:10.1038/nrm2330 Medline
26. D. L. Valentine, Adaptations to energy stress dictate the ecology and evolution of the Archaea. *Nat. Rev. Microbiol.* **5**, 316–323 (2007). doi:10.1038/nrmicro1619 Medline
27. Y.-Y. Chang, J. E. Cronan Jr., Membrane cyclopropane fatty acid content is a major factor in acid resistance of Escherichia coli. *Mol. Microbiol.* **33**, 249–259 (1999). doi:10.1046/j.1365-2958.1999.01456.x Medline
28. D. Milenkovic, J. N. Blaza, N. G. Larsson, J. Hirst, The Enigma of the Respiratory Chain Supercomplex. *Cell Metab.* **25**, 765–776 (2017). doi:10.1016/j.cmet.2017.03.009 Medline
29. J. A. Letts, K. Fiedorczuk, L. A. Sazanov, The architecture of respiratory supercomplexes. *Nature* **537**, 644–648 (2016). doi:10.1038/nature19774 Medline
30. J. W. Campbell, J. E. Cronan Jr., Escherichia coli FadR positively regulates transcription of the fabB fatty acid biosynthetic gene. *J. Bacteriol.* **183**, 5982–5990 (2001). doi:10.1128/JB.183.20.5982-5990.2001 Medline
31. H. J. Cha Srivastava, R., Vakharia, V., Rao, G., and W. E. Bentley, Green fluorescent protein as a non-invasive "stress probe" in resting recombinant Escherichia coli

Downloaded from http://science.sciencemag.org/ on October 25, 2018

culture. *Appl. Environ. Microbiol.* **65**, 409–414 (1999).
32. R. W. Haushalter, W. Kim, T. A. Chavkin, L. The, M. E. Garber, M. Nhan, P. D. Adams, C. J. Petzold, L. Katz, J. D. Keasling, Production of anteiso-branched fatty acids in Escherichia coli; next generation biofuels with improved cold-flow properties. *Metab. Eng.* **26**, 111–118 (2014). doi:10.1016/j.ymben.2014.09.002 Medline
33. H. Alper, C. Fischer, E. Nevoigt, G. Stephanopoulos, Tuning genetic control through promoter engineering. *Proc. Natl. Acad. Sci. U.S.A.* **102**, 12678–12683 (2005). doi:10.1073/pnas.0504604102 Medline
34. D. Degreif, T. de Rond, A. Bertl, J. D. Keasling, I. Budin, Lipid engineering reveals regulatory roles for membrane fluidity in yeast flocculation and oxygen-limited growth. *Metab. Eng.* **41**, 46–56 (2017). doi:10.1016/j.ymben.2017.03.002 Medline
35. R. Herzog, K. Schuhmann, D. Schwudke, J. L. Sampaio, S. R. Bornstein, M. Schroeder, A. Shevchenko, LipidXplorer: A software for consensual cross-platform lipidomics. *PLOS ONE* **7**, e29851 (2012). doi:10.1371/journal.pone.0029851 Medline
36. M. Bekker, G. Kramer, A. F. Hartog, M. J. Wagner, C. G. de Koster, K. J. Hellingwerf, M. J. de Mattos, Changes in the redox state and composition of the quinone pool of Escherichia coli during aerobic batch-culture growth. *Microbiology* **153**, 1974–1980 (2007). doi:10.1099/mic.0.2007/006098-0 Medline
37. T. S. Batth, P. Singh, V. R. Ramakrishnan, M. M. L. Sousa, L. J. G. Chan, H. M. Tran, E. G. Luning, E. H. Y. Pan, K. M. Vuu, J. D. Keasling, P. D. Adams, C. J. Petzold, A targeted proteomics toolkit for high-throughput absolute quantification of Escherichia coli proteins. *Metab. Eng.* **26**, 48–56 (2014). doi:10.1016/j.ymben.2014.08.004 Medline
38. A. Kubalski, Generation of giant protoplasts of Escherichia coli and an inner-membrane anion selective conductance. *Biochim. Biophys. Acta* **1238**, 177–182 (1995). doi:10.1016/0005-2736(95)00126-N Medline
39. D. E. Koppel, M. P. Sheetz, M. Schindler, Lateral diffusion in biological membranes. A normal-mode analysis of diffusion on a spherical surface. *Biophys. J.* **30**, 187–192 (1980). doi:10.1016/S0006-3495(80)85087-9 Medline
40. A. Milon, J. Ricka, S.-T. Sun, T. Tanaka, Y. Nakatani, G. Ourisson, Precise determination of the hydrodynamic radius of phospholipid vesicles near the phase transition. *Biochim. Biophys. Acta* **777**, 331–333 (1984). doi:10.1016/0005-2736(84)90435-8
41. C. Burstein, L. Tiankova, A. Kepes, Respiratory control in Escherichia coli K 12. *Eur. J. Biochem.* **94**, 387–392 (1979). doi:10.1111/j.1432-1033.1979.tb12905.x Medline
42. V. B. Borisov, R. Murali, M. L. Verkhovskaya, D. A. Bloch, H. Han, R. B. Gennis, M. I. Verkhovsky, Aerobic respiratory chain of Escherichia coli is not allowed to work in fully uncoupled mode. *Proc. Natl. Acad. Sci. U.S.A.* **108**, 17320–17324 (2011). doi:10.1073/pnas.1108217108 Medline
43. P. Munujos, J. Coll-Cantí, F. González-Sastre, F. J. Gella, Assay of succinate dehydrogenase activity by a colorimetric-continuous method using iodonitrotetrazolium chloride as electron acceptor. *Anal. Biochem.* **212**, 506–509 (1993). doi:10.1006/abio.1993.1360 Medline
44. K. Matsushita, T. Ohnishi, H. R. Kaback, NADH-ubiquinone oxidoreductases of the Escherichia coli aerobic respiratory chain. *Biochemistry* **26**, 7732–7737 (1987). doi:10.1021/bi00398a029 Medline
45. C. E. VanOrsdel, S. Bhatt, R. J. Allen, E. P. Brenner, J. J. Hobson, A. Jamil, B. M. Haynes, A. M. Genson, M. R. Hemm, The Escherichia coli CydX protein is a member of the CydAB cytochrome bd oxidase complex and is required for cytochrome bd oxidase activity. *J. Bacteriol.* **195**, 3640–3650 (2013). doi:10.1128/JB.00324-13 Medline
46. S. J. Koepke, J. J. Watkins, S. D. Minteer, Understanding the Role of Mitochondrial Health in the Mechanism of Mitochondrial Bioelectrocatalysis. *J. Electrochem. Soc.* **163**, H292–H298 (2016). doi:10.1149/2.0681605jes
47. G. W. Rogers, M. D. Brand, S. Petrosyan, D. Ashok, A. A. Elorza, D. A. Ferrick, A. N. Murphy, High throughput microplate respiratory measurements using minimal quantities of isolated mitochondria. *PLOS ONE* **6**, e21746 (2011). doi:10.1371/journal.pone.0021746 Medline
48. K. Kita, K. Konishi, Y. Anraku, Terminal oxidases of Escherichia coli aerobic respiratory chain. I. Purification and properties of cytochrome b562-o complex from cells in the early exponential phase of aerobic growth. *J. Biol. Chem.* **259**, 3368–3374 (1984). Medline
49. D. Shoup, A. Szabo, Role of diffusion in ligand binding to macromolecules and cell-bound receptors. *Biophys. J.* **40**, 33–39 (1982). doi:10.1016/S0006-3495(82)84455-X Medline
50. H. C. Berg, E. M. Purcell, Physics of chemoreception. *Biophys. J.* **20**, 193–219 (1977). doi:10.1016/S0006-3495(77)85544-6 Medline
51. J. Keizer, J. Ramirez, E. Peacock-López, The effect of diffusion on the binding of membrane-bound receptors to coated pits. *Biophys. J.* **47**, 79–87 (1985). doi:10.1016/S0006-3495(85)83879-0 Medline
52. D. A. Lauffenburger, J. Linderman, *Receptors: models for binding, trafficking, and signaling* (Oxford University Press, 1993).
53. T. Althoff, D. J. Mills, J.-L. Popot, W. Kühlbrandt, Arrangement of electron transport chain components in bovine mitochondrial supercomplex I1III2IV1. *EMBO J.* **30**, 4652–4664 (2011). doi:10.1038/emboj.2011.324 Medline
54. E. Lapuente-Brun, R. Moreno-Loshuertos, R. Acín-Pérez, A. Latorre-Pellicer, C. Colás, E. Balsa, E. Perales-Clemente, P. M. Quirós, E. Calvo, M. A. Rodríguez-Hernández, P. Navas, R. Cruz, Á. Carracedo, C. López-Otín, A. Pérez-Martos, P. Fernández-Silva, E. Fernández-Vizarra, J. A. Enríquez, Supercomplex assembly determines electron flux in the mitochondrial electron transport chain. *Science* **340**, 1567–1570 (2013). doi:10.1126/science.1230381 Medline
55. J. N. Blaza, R. Serreli, A. J. Y. Jones, K. Mohammed, J. Hirst, Kinetic evidence against partitioning of the ubiquinone pool and the catalytic relevance of respiratory-chain supercomplexes. *Proc. Natl. Acad. Sci. U.S.A.* **111**, 15735–15740 (2014). doi:10.1073/pnas.1413855111 Medline
56. N. Oppenheimer, H. A. Stone, Effect of Hydrodynamic Interactions on Reaction Rates in Membranes. *Biophys. J.* **113**, 440–447 (2017). doi:10.1016/j.bpj.2017.06.013 Medline
57. D. Marchal, W. Boireau, J. M. Laval, J. Moiroux, C. Bourdillon, Electrochemical measurement of lateral diffusion coefficients of ubiquinones and plastoquinones of various isoprenoid chain lengths incorporated in model bilayers. *Biophys. J.* **74**, 1937–1948 (1998). doi:10.1016/S0006-3495(98)77902-0 Medline
58. A. Nenninger, G. Mastroianni, A. Robson, T. Lenn, Q. Xue, M. C. Leake, C. W. Mullineaux, Independent mobility of proteins and lipids in the plasma membrane of Escherichia coli. *Mol. Microbiol.* **92**, 1142–1153 (2014). doi:10.1111/mmi.12619 Medline
59. R. Peters, R. J. Cherry, Lateral and rotational diffusion of bacteriorhodopsin in lipid bilayers: Experimental test of the Saffman-Delbrück equations. *Proc. Natl. Acad. Sci. U.S.A.* **79**, 4317–4321 (1982). doi:10.1073/pnas.79.14.4317 Medline
60. P. Cicuta, S. L. Keller, S. L. Veatch, Diffusion of liquid domains in lipid bilayer membranes. *J. Phys. Chem. B* **111**, 3328–3331 (2007). doi:10.1021/jp0702088 Medline
61. Y. Gambin, R. Lopez-Esparza, M. Reffay, E. Sierecki, N. S. Gov, M. Genest, R. S. Hodges, W. Urbach, Lateral mobility of proteins in liquid membranes revisited. *Proc. Natl. Acad. Sci. U.S.A.* **103**, 2098–2102 (2006). doi:10.1073/pnas.0511026103 Medline
62. N. A. Newton, G. B. Cox, F. Gibson, Function of ubiquinone in Escherichia coli: A mutant strain forming a low level of ubiquinone. *J. Bacteriol.* **109**, 69–73 (1972). Medline
63. K. Kita, K. Konishi, Y. Anraku, Terminal oxidases of Escherichia coli aerobic respiratory chain. II. Purification and properties of cytochrome b558-d complex from cells grown with limited oxygen and evidence of branched electron-carrying systems. *J. Biol. Chem.* **259**, 3375–3381 (1984). Medline
64. M. Braun, S. Bungert, T. Friedrich, Characterization of the overproduced NADH dehydrogenase fragment of the NADH:ubiquinone oxidoreductase (complex I) from Escherichia coli. *Biochemistry* **37**, 1861–1867 (1998). doi:10.1021/bi971176p Medline
65. K. Björklöf, V. Zickermann, M. Finel, Purification of the 45 kDa, membrane bound NADH dehydrogenase of Escherichia coli (NDH-2) and analysis of its interaction with ubiquinone analogues. *FEBS Lett.* **467**, 105–110 (2000). doi:10.1016/S0014-5793(00)01130-3 Medline
66. E. Maklashina, T. M. Iverson, Y. Sher, V. Kotlyar, J. Andréll, O. Mirza, J. M. Hudson, F. A. Armstrong, R. A. Rothery, J. H. Weiner, G. Cecchini, Fumarate reductase and succinate oxidase activity of Escherichia coli complex II homologs are perturbed differently by mutation of the flavin binding domain. *J. Biol. Chem.* **281**, 11357–11365 (2006). doi:10.1074/jbc.M512544200 Medline
67. V. Sharma, J. Eckels, G. K. Taylor, N. J. Shulman, A. B. Stergachis, S. A. Joyner, P. Yan, J. R. Whiteaker, G. N. Halusa, B. Schilling, B. W. Gibson, C. M. Colangelo, A. G. Paulovich, S. A. Carr, J. D. Jaffe, M. J. MacCoss, B. MacLean, Panorama: A targeted

Downloaded from http://science.sciencemag.org/ on October 25, 2018

proteomics knowledge base. *J. Proteome Res.* **13**, 4205–4210 (2014). doi:10.1021/pr5006636 Medline
68. J. Suurkuusk, B. R. Lentz, Y. Barenholz, R. L. Biltonen, T. E. Thompson, A calorimetric and fluorescent probe study of the gel-liquid crystalline phase transition in small, single-lamellar dipalmitoylphosphatidylcholine vesicles. *Biochemistry* **15**, 1393–1401 (1976). doi:10.1021/bi00652a007 Medline

ACKNOWLEDGMENTS

Naomi Oppenheimer, Howard Stone, and Dan Arlow contributed helpful discussions and the Coates (University of California, Berkley) and Lippincott-Schwartz (Janelia Research Campus) labs contributed experimental assistance. **Funding:** This work was part of the DOE Joint BioEnergy Institute supported by the U. S. Department of Energy, Office of Science, Office of Biological and Environmental Research, through contract DE-AC02-05CH11231 between Lawrence Berkeley National Laboratory and the U. S. Department of Energy. This work was also supported by National Science Foundation grants MCB-1442724 and MCB-1715681 to J.D.K, and a Junior Fellowship to I.B. from the Miller Institute for Basic Research. **Author contributions:** I.B. designed the study and performed the experiments. T.d.R. developed the model with I.B. and performed chemical synthesis. Y.C., LJ.G.C., and C.J.P. performed protein mass spectrometry analysis. All authors wrote the paper and discussed the results. **Competing interests:** J.D.K. has a financial interest in Amyris, Lygos, Demetrix, Constructive Biology, Maple Bio, and Napigen. The research described in this publication is not related to the work of these companies. **Data and material availability:** All strains are available from the Joint BioEnergy Institute public registry (https://public-registry.jbei.org). Protein mass spectrometry SRM data and methods are available at Panamoramaweb (http://goo.gl/JJySak). The ETC simulation script, written in Python, as well as examples of commands to invoke it, are available at GitHub (http://github.com/tderond/Budin2018).

SUPPLEMENTARY MATERIALS

www.sciencemag.org/cgi/content/full/science.aat7925/DC1
Materials and Methods
Supplementary Text
Figs. S1 to S11
Tables S1 to S3
References (*30-68*)
Movies S1 and S2

5 April 2018; accepted 11 October 2018
Published online 25 October 2018
10.1126/science.aat7925

Downloaded from http://science.sciencemag.org/ on October 25, 2018

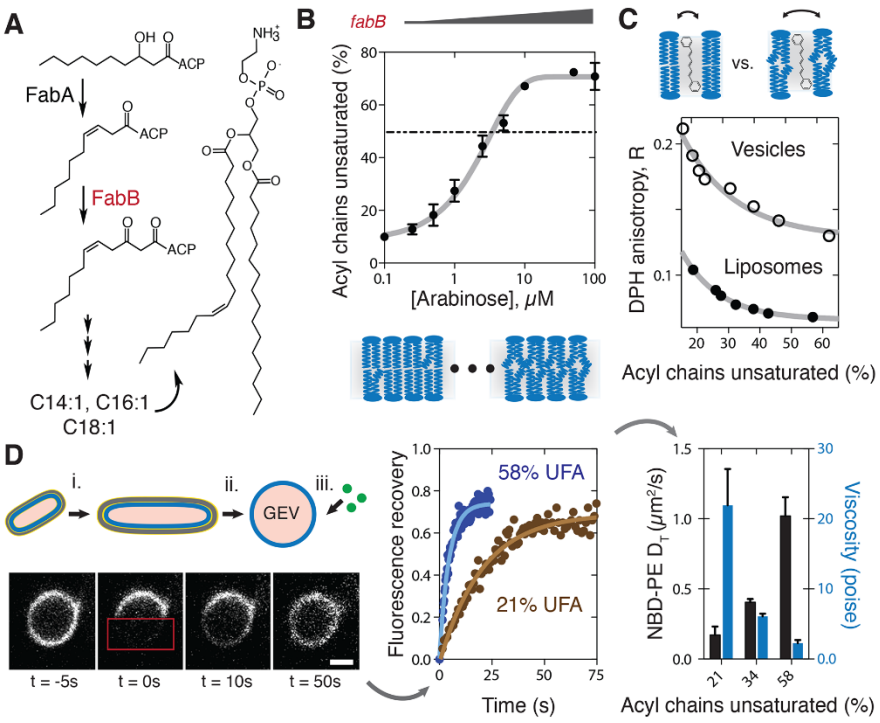

Fig. 1. Genetic titration of inner membrane viscosity in *E. coli*. (**A**) The pathway for bacterial UFA synthesis. The activity of FabB is rate-limiting for UFA synthesis and incorporation into phospholipids. (**B**) Titration of *fabB* expression with the P_{BAD} promoter modulates UFA stoichiometry as a function of inducer (arabinose) concentration. This leads to membranes with increasing amounts of *cis* double bonds, as shown in the model. Data are mean +/− SD (*N* = 3). (**C**) Characterization of membrane ordering using DPH anisotropy. Higher anisotropy values indicate restricted motion of the probe and therefore a more ordered membrane. (**D**) A FRAP-based assay for measuring inner membrane diffusivities and its application in estimating membrane microviscosity. GEVs were generated by elongating cells with cephalexin (*i*). Cell walls were then digested (*ii*), thereby generating large, inner membrane vesicles to which lipid fluorophores can be added externally (*iii*). Shown is an experiment for a model substrate, NBD-PE, with recovery curves for two lipid compositions. Translational diffusion coefficients (D_T) were generated from the exponential constant of the recovery curve and viscosity values were then estimated from these. Black bars show the calculated diffusion coefficients for NBD-PE (left Y-axis), and blue bars show the extrapolated estimated membrane viscosity (right Y-axis). Data are mean +/− SEM (*N* = 5).

Downloaded from http://science.sciencemag.org/ on October 25, 2018

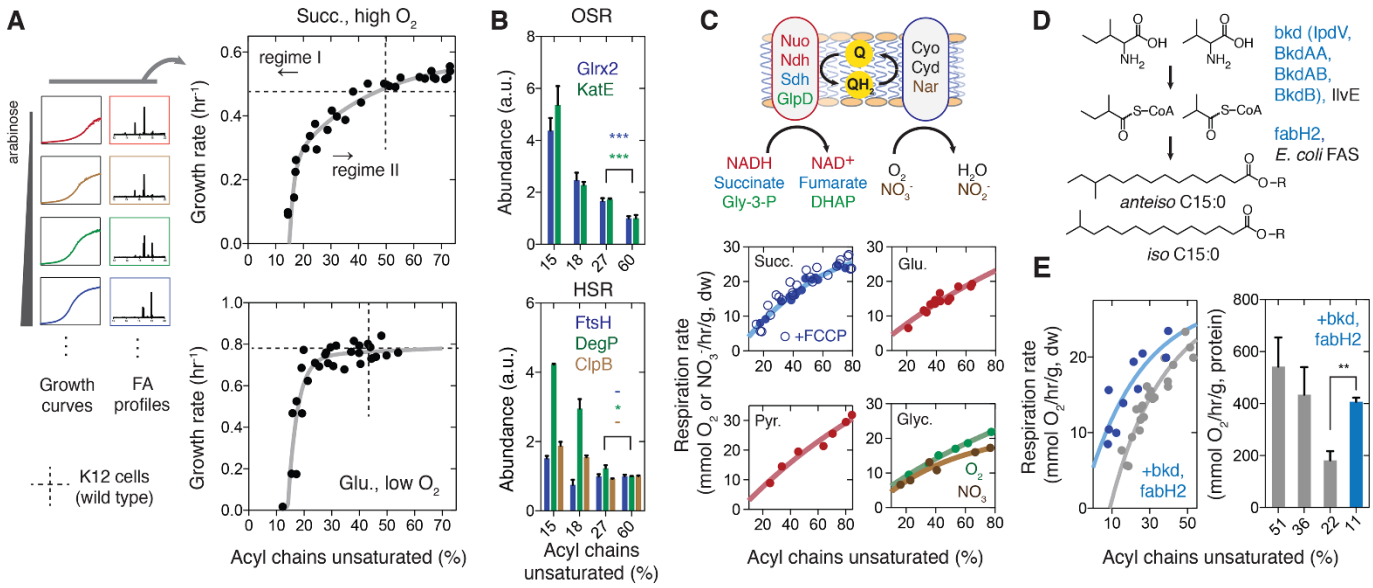

Fig. 2. Effects of fatty acid composition on physiology and respiratory metabolism. (**A**) Growth rates and FA compositions were characterized for a series of batch cultures with various arabinose concentrations. The growth rate dependence on UFA levels occurs in two phases: a fitness cliff at low levels (regime I), and a gradual increase in growth rates at intermediate levels (regime II); these can be described by two exponential constants: $k_1 \sim 0.6\%^{-1}$, $k_2 \sim 0.03\%^{-1}$ at 37°C. The top plot shows the growth rate dependence under respiratory conditions (succinate, high oxygen) while the bottom shows it for fermentative conditions (glucose, low oxygen), when regime II is absent. (**B**) Abundance of stress response factors in response to different proportions of unsaturated acyl chains. Data are mean +/− SEM (N = 3) and overlaid are the results of t tests for significance between abundances in high (60%) and intermediate (27%) lipid unsaturation. ***, $p < 0.001$; *, $p < 0.05$, -, no significance. (**C**) The modular *E. coli* ETC consists of dehydrogenase (red) and terminal oxidase (blue) enzymes that react via an intermediate quinone pool. The different enzyme complexes utilized are color coded according to substrate. The corresponding respiration rates, as measured by oxygen or nitrate consumption, show a similar dependence ($k \sim 0.01$-$0.03\%^{-1}$) on lipid unsaturation regardless of the electron donor or acceptor and whether the ETC is uncoupled by carbonyl cyanide-4-(trifluoromethoxy)phenylhydrazone (FCCP). (**D**) Heterologous biosynthesis of *anteiso* and *iso* BCFAs from amino acid precursors in *E. coli* using genes (highlighted in blue) from *B. subtilis*. (**E**) Effects of BCFA biosynthesis on uncoupled succinate respiration rates with various levels of lipid unsaturation (left). In purified membrane vesicles (right), the abundance of unsaturated fatty acids also mediates succinate respiration and a UFA deficiency can be rescued by BCFA biosynthesis, which increases respiration rates in UFA-depleted membranes (t test for significance $p = 0.002$, **). Data are mean +/− SEM (N = 3).

Downloaded from http://science.sciencemag.org/ on October 25, 2018

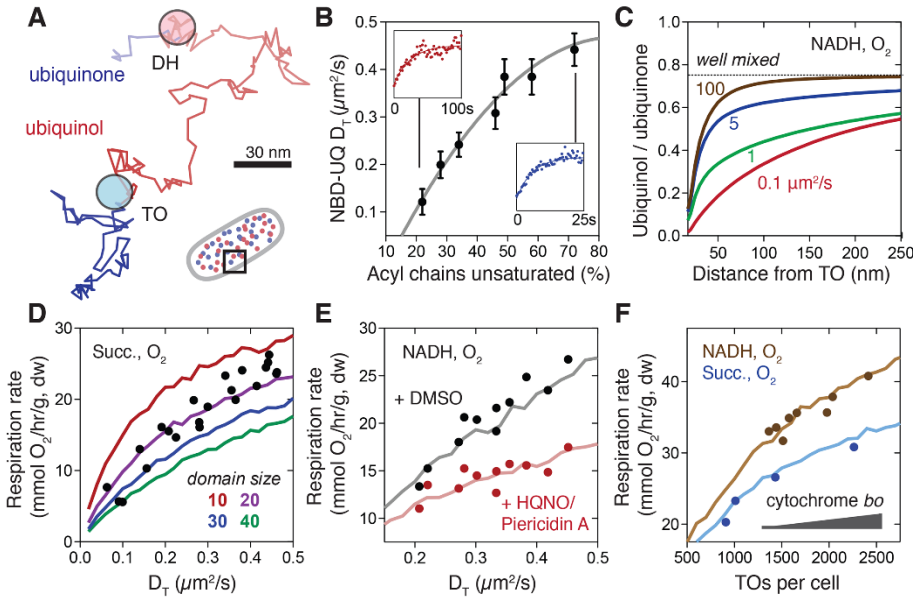

Fig. 3. Testing a diffusion-coupled reaction model for bacterial respiration. (**A**) A simulated random walk by a ubiquinone, which becomes reduced to ubiquinol (red) upon interaction with a DH domain and then re-oxidized (blue) upon subsequent collisions with a TO, an oxygen consuming reaction. The opacity of the path indicates progression during the time course (100 ms). (**B**) Experimental measurements of ubiquinone diffusivity in GEVs. Values are shown as averages from eight GEVs for each preparation. Solid line shows a quadratic function fit to the data, and is used as a standard curve to convert lipid composition to diffusivity in subsequent experiments. Inserts show example FRAP exponential recovery curves. Data are mean +/− SEM (*N* =5). (**C**) The distribution of the ubiquinone pool as a function of its diffusivity in whole cell simulations, expressed as the steady-state average ubiquinol:ubiquinone ratio within a given radius of a TO. (**D**) Comparison of the simulated dependence of ubiquinone diffusivity (D_T) on respiration rates (solid lines) with measurements of uncoupled respiration in succinate medium (dots). Values in the legend are the domain size of the modeled ETC enzyme pair. (**E**) Modeling the effect of reducing enzymatic activity using the inhibitors N-oxo-2-heptyl-4-hydroxyquinoline (HQNO) and piericidin A, which act on TOs and NADH DH, respectively. Simulated rates of NADH-linked respiration (solid lines), modeled using 20-mer homotypic domains, are shown alongside uncoupled respiration rates in pyruvate medium (dots) under various UFA levels with HQNO (20 μM) and piericidin A (100 nM), or with no inhibitors (DMSO). (**F**) The effect of changes in TO concentration – achieved by titrating expression of *cyoABCD* – on respiratory rates. Simulation results (solid lines) are superimposed with experimental measurements of NADH respiration with pyruvate (brown) and succinate respiration (blue); measured TO abundance includes both aerobic cytochrome oxidases (*bo* and *bd*-I).

Downloaded from http://science.sciencemag.org/ on October 25, 2018

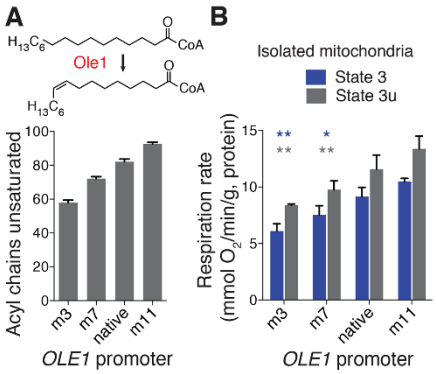

Fig. 4. Lipid-mediated respiration in mitochondria. (**A**) The desaturase Ole1 generates all UFAs in yeast. Unsaturated lipid composition is controlled by the promoter driving expression of *OLE1* - either the native one, or one of three variants (m3, m7, m11) in engineered strains. (**B**) Mitochondrial respiration rates in coupled (State 3, 0.5 mM ADP) and uncoupled (State 3u, 4 μM FCCP) conditions corresponded with unsaturated lipid content. Mitochondria were incubated with 5 mM succinate as a substrate. Data are mean +/− SEM (*N* = 3) and overlaid are the results of *t* tests for significance against m11. **, $p < 0.01$; *, $p < 0.05$.

Downloaded from http://science.sciencemag.org/ on October 25, 2018

Science

Viscous control of cellular respiration by membrane lipid composition

Itay Budin, Tristan de Rond, Yan Chen, Leanne Jade G. Chan, Christopher J. Petzold and Jay D. Keasling

published online October 25, 2018

ARTICLE TOOLS http://science.sciencemag.org/content/early/2018/10/24/science.aat7925

SUPPLEMENTARY MATERIALS http://science.sciencemag.org/content/suppl/2018/10/24/science.aat7925.DC1

REFERENCES This article cites 67 articles, 25 of which you can access for free
http://science.sciencemag.org/content/early/2018/10/24/science.aat7925#BIBL

PERMISSIONS http://www.sciencemag.org/help/reprints-and-permissions

Use of this article is subject to the Terms of Service

Science (print ISSN 0036-8075; online ISSN 1095-9203) is published by the American Association for the Advancement of Science, 1200 New York Avenue NW, Washington, DC 20005. 2017 © The Authors, some rights reserved; exclusive licensee American Association for the Advancement of Science. No claim to original U.S. Government Works. The title *Science* is a registered trademark of AAAS.

Downloaded from http://science.sciencemag.org/ on October 25, 2018